The Microstructure and the Wear Performance of High Carbon Ferrochrome *Fecrv15* and *Fecrv15+cr* Manufacture Through Laser Additive Manufacturing on Steel Baseplate for Tillage Application

Basiru Philip Aramide (abashiruphilip@gmail.com)
Tshwane University of Technology https://orcid.org/0000-0002-6488-1287
Rotimi E Sadiku
Tshwane University of Technology
Patricia A Popoola
Tshwane University of Technology
Sisa L Pityana
Council for Scientific and Industrial Research
Tamba Jamiru
Tshwane University of Technology

Research Article

Keywords: Microstructural modification, laser additive manufacturing, chromium addition, In-situ, wear performance

Posted Date: January 19th, 2022

DOI: https://doi.org/10.21203/rs.3.rs-1166508/v1

Abstract

The enhancement of wear performance of steel baseplate for tillage application was carried out by manufacturing vanadium-chromium carbide coatings in situ by powder infusion of high carbon ferrochrome FeCrV15 powder through laser additive manufacturing. The developed samples were subjected to various microstructural investigations, microhardness and wear tests. The effect of extra chromium addition was also investigated on the developed coatings' microstructure, hardness and wear performance. It was observed that the extra chromium addition increased the austenitic iron formation, reduced the concentration of the precipitated carbides and resulted in a much bigger grain formation of phases present, which lowered the grain boundary density leading to a reduced hardness of 553 HV for FeCrV15+Cr, compared to 835 HV for FeCrV15; which are significantly higher than 170 HV for the steel substrate. The result produced defect-free coatings with a strong metallurgical bond to the substrate. The FeCrV15 coating displayed an improved, multiple times wear-resistant capacity when contrasted with the FeCrV15+Cr. This excellent resistance is credited to the increased concentration of VC–Cr_3C_3 particles and increased grain boundary density due to the grain refinement of FeCrV15 coating, which are emphatically fortified in the matrix.

1. Introduction

In the present innovative world, tillage tools with high resistance to wear and corrosion are needed for soil cultivating machines because of their relatively high velocity in the relatively moving mass of soil. The low-composite, high carbon, and medium carbon steel material are utilised to produce the tillage tools for soil preparation because of their excellent sturdiness, high strength and abundant availability. The material loss occurs due to abrasive wear brought about by the scouring of hard particles from the soil on the face of tillage material and the relatively high velocity of soil-tools movement [1, 2]. The working pieces of cultivating machines, soil cultivators, smashers, and mining machines are presented to dynamic stacking and chemical substances present in the soil [3, 4], which causes misfortune and damages to the instrument materials. Wear of tillage tools during land cultivation brings about higher power requirements, ceaseless personal times for substitution of worn tools, and higher costs for machinery operations. According to Natsis et al. [5], it was discovered in a field test that the ploughshare thickness influences the fuel utilisation and draft powers or forces of a tractor. It was discovered that increasing the thickness of ploughshare from 1 to 6 mm improved tractor fuel consumption by 41%, draft power improved by 62%, and work rate reduced by 30%. The tools' material needs to be of high strength and must be highly resistant to abrasive wear because of its direct contact with hard grating particles of the soil. Although wear cannot be totally eliminated, it could be compelled by some sensible advances to a reasonable level [2]. Intending to do this, scientists are examining and investigating strategies of lowering the frictional obstruction between tillage instruments and the soil.

Hard coatings have been used to limit the wear rates and upgrade the toughness of tillage tools [2, 6]. Scientists recently attempted to improve the toughness and wear resistance of tillage tools through various hard coatings procedures. Kang et al. [7] analysed wear reactions of three thermally sprayed

coating powders (Cr3C2-NiCr, WCCo-Cr, and Stellite-21) on EN-14B steel used for rotary tiller blades. It was seen that WC-Co-Cr has the most outstanding wear resistance, trailed by Cr3C2-NiCr and Stellite-21, respectively, when contrasted with the substrate. Hrabe and Muller [8] investigated the wear reaction of three particular hard coatings on ploughshares (the powders utilised are WC-Co based, high chromium-based and Cr-Nb based). A ploughshare with no coatings was used as a control. The wear rate of coated ploughshare was observed to decrease during the field test compared to the standard ploughshare. Reduced weight reduction was seen in WC-Co based hard coating in contrast with high chromium- and Cr-Nb based hard coatings. Horvat et al. [9] study the furrowing effectiveness and wear reaction of ploughshares produced using manganese steel (50Mn7) and ploughshare covered with CCo-Cr-Ni-Si compound coatings in field condition. The wear rate of covered ploughshare diminished due to the presence of hard carbide of chromium, which is essentially harder than SiO2 generally present in the soil. It was found that this upgrade in wear resistance of covered ploughshares decreased fuel use of tractors by 7 to 8% more than common ploughshares.

Previous studies have revealed that Vanadium-chromium carbide's precipitation upgraded the microstructure, grain refinement, and hardness of reinforced FeCrV15 hardfacing laser coated steel plate [10, 11]. The extra addition of chromium to the coating increased the formation of austenitic iron, lowered the hardness of the reinforced coatings [12, 13], reduced the polarisation potential, increased the corrosion current density and raised the corrosion rate to a higher value. The present study investigates the impact of these observed effects in the microstructure and hardness on wears performances of the coatings.

2. Materials And Methods

2.1 Materials and the Processing Equipment

High carbon ferrochrome (FeCrV15) powder of the particle size distribution of -150 +50 μm were hard-faced both separately and combined in-situ with chromium [14] powders on steel base plate with dimensions 100mm x100 mm x 5mm through laser cladding process. The powder materials used for the study were both supplied by the WearTech of South Africa and Samaterial of the United States, respectively, at purity of as received above 99%, see Fig. 1. The materials were utilised as received without modification. Table 1 represents the weight composition of the materials used for the study. The samples with their processing parameters are presented in Table 2; these parameters were fully optimised before this study [10, 12, 15].

Table 1
The elemental weight composition of the powders and the baseplate

Elements	C	Mo	Mn	O	Cr	Si	V	Al	Fe
FeCrV15	4.5	1.3	1.1	-	14.0	1.1	15.4	-	Balance
Chromium	3.62	-	-	8.00	Balance	-	-	-	-
Baseplate	2.54	-	1.32	-	-	0.12	-	0.17	Balance

Table 2
The samples, coating powders and their processing parameters

Samples	Laser Beam power (W)	Scanning speed (mm/s)	Powder used	Powder feed rate (g/min)
A	1200	8	FeCrV15	5
B	1200	8	FeCrV15 + Cr	5 + 0.4

The surface of the substrate was sandblasted and appropriately cleaned with acetone to remove contamination, reduce reflection and improve absorptivity of the laser beam light. The laser cladding deposition of five tracts with three layers and 50% overlap was carried out using 3kW Continuous Wave (CW) IPG Fibre laser system. The DPSF-2 type coaxial powder feeder was used to dispense powder in-situ to the substrate assisted by argon as both the shielding and carrying gas at a flow rate of 15L/min and 2L/min, respectively. The schematic diagram of the laser head and process is shown in Fig. 2.

2.2 Physical Characterisation and Image Processing

Before the microstructure was examined, the samples were first ground and polished, progressively utilising the Silicon carbide paper from 80, 380, 1200, and 1400 coarse sandpapers. Test surfaces were afterwards polished on a polished disc with 1μm, 0.9μm and 0.3μm alumina powder to attain a mirror surface of all samples. Two different etchants were tried out, and the one with the best outcome was utilised on the second batch of the samples, which resulted in a slight difference between samples. Different samples were then analysed with an Optical Polarizing Microscope (OPM) and Scanning Electron Microscope equipped with Energy Dispersive Spectroscopy (SEM/EDS). XRD investigation was done on the coatings utilising Cu Kα1 radiation.

2.3 Mechanical Characterisation

The mechanical response of the coatings was also examined. The hardness, coefficient of friction (COF), wear rate and wear resistance to abrasion were among the factors examined. Vickers microhardness tester, with a load of 300 g and a dwelling time of 10s, was used to take the hardness of the coatings beginning at the top surface, which was repeated three times, and the average determined. The reading was taken every 0.2mm until the core of the substrate was reached.

The Anton Paar Tribometer, with a silicon nitride ball of 1.5 mm radius, was used to conduct the abrasive wear experiment to determine the coefficient of friction (COF) and wear rate (see Fig. 3). The load used is 20N, with a 200rpm speed; the operating time of 30min was adopted for the investigation. The wear rate was acquired by a profilometer which did profile the wear track. The image of the wear track was acquired utilising the SEM/EDS.

3. Results Analysis And Discussion

3.1 The clads microstructures and their characteristic

The micrographs of the coatings are presented in **Fig.4** (A, B, & C represent Sample **A**, while D, E, & F represent Sample **B**). The images were taken beginning from the portion of the clads closer to the substrates and progressively to the topmost portion far away from the substrate.

From the images presented and as reported by [10, 17], the white spots (**Fig. 4A** & **D**) all over the microstructure represent the precipitation of vanadium carbides, VCs. Which is eutectic, and it is predominant in the first layer of the clad. In addition to the remelting of the precipitated VCs from the previously cladded layer, more melted powders are fed into the melt pool as the subsequent layers are being built, this increases the concentration of the precipitated VCs in both samples, which began to agglomerate [11] into more prominent and starlike grains of primary VCs (see **Fig. 4B, C**, **E**, and **F**). The iron and Cr-rich carbide was observed to fill the grain boundaries with dark martensitic phases lammed through the micrograph (see **Fig. 4A** and **B**). The further away from the substrate into the clad, the bigger the grain size of the primary VC and the lower the concentration of the eutectic VC [17] for both samples. The concentration of primary VC, eutectic VC and Cr-rich carbides in sample A (see **Fig. 4A, B**, and **C**) are more than sample B (see **4D**, **E**, and **F**) as observed in the micrographs; moreover, the formation of the grains of sample A is more refined and more petite than sample B, see Fig. 5c and 5d respectively. This was reported by Aramide et al. [13] as the effect of extra chromium addition, which increased the austenitic iron (γFe) and chromium element formation in the matrix and resulted in bigger grains formation in sample B; it was also asserted to reduce the formation and precipitation of primary VCs, eutectic VCs and Cr-rich carbides. This is responsible for the reduced concentration of the VCs and Cr-rich carbides in sample B, which is confirmed by the lowered peaks of the precipitated carbides, and higher peaks of the austenites in sample B compared to sample A in the presented X-ray diffractometry result in Figure 6 [12].

3.2 Microhardness

The clad sample's hardness depends on the percentage concentration of the precipitated carbide phases [18, 19] and the grain refinement of the phases present [20] in the microstructure. As stated earlier, the hardness was measured at an interval of 0.2 mm from the top of the clad with a load of 300 g and a dwelling time of 10 s until the substrate's core is reached, see Fig. 7. The microhardness of both coatings has a vast improvement than the steel substrate, although sample B has a relatively low hardiness value of 553 HV 0.3 than sample A, which has an average hardness of 835 HV 0.3, which are far better than the

steel substrate, with an average microhardness value of 170 HV 0.3. The significantly high microhardness values of clads can be explained by the formation and the precipitation of hard VC-Cr_3C_2 in the microstructures of the coatings [16]. In addition, and as explained in the previous section, the grain refinement in the microstructure of sample A resulted in a higher concentration of VC-Cr_3C_2 precipitates, which invariably increases the sample's grain boundary density [20], resulting in its higher microhardness value compared to sample B.

The hardness of the interface between the substrate and coating was higher than any other portion for sample B. This higher value of microhardness is probably credited to the confined martensitic phase transformation in the heat-affected zone (HAZ), resulting from the rapid heating and cooling effect with a temperature higher than the phase transformation temperature of this particular steel but lower than its melting point [16].

3.3 Wear performance of the clads

The representation of the dry sliding wear experimentation of both coatings carried out at room temperature is shown in Fig. 8. Sample A exhibits a wear resistance that is approximately 6 times higher than sample B. The friction coefficient variation of both clad coatings as a function of time under the dry sliding test condition is represented in Fig. 9. It shows that the coefficient of friction for sample A, is about 0.4 and 0.65 at the beginning for sample B, which later reduces to about 0.5. Moreover, the friction coefficient for sample B exhibits a higher fluctuation than sample A.

To better understand the worn surfaces, the micrographs are presented in **Fig. 10**. A seriously worn surface was observed in sample B (FeCrV15+Cr coating), with deep grooves, while in sample A (FeCrV15 coating), a relatively smooth surface with minor scratches were observed compared to sample B. It is noticeable that, under a dry-sliding condition with high sliding speed, contact shearing was excessively quick such that frictional heat was produced at a rate a lot quicker than it could be conducted away. Thus, with high sliding velocity, the high heat delivered a severe grip on the counter surfaces, consequently increasing the coefficient of friction radically, prompting an increased wear rate [21]. The wear mechanism in the multiphase composites is exceptionally complicated, contingent on a few factors: volume fraction, distribution, the morphology of the ceramic particles, the grain refinement of formed phases, and wear condition [22].

In any case, the dominant wear mechanism of the in-situ VC-Cr_3C_2 reinforced coatings under this wear test experiment can be described as a combination of micro-polishing and adhesion mechanisms. The matrix phase γ-Fe with low hardness in the hard-faced coatings go through metal-ceramic contact with the mating wheel at a high sliding rate, demonstrating adhesion can occur between the tribo-surfaces, which additionally brings about the resulting material transfer. This, thus, prompts the exposure of VC–Cr_3C_2 particles to the steel countersurface. Subsequently, VC–Cr_3C_2 particles with high hardness can adequately withstand the load and assume a significant role in opposing plastic deformation of the coatings because of the frictional heat generated due to dry-sliding between the coatings and tribometer. However, the longer the load lingered on the samples, B began to give way; deep and continuous grooves

were observed on it, whereas shallow and discontinuous grooves could be seen on sample A. Moreover the wear debris on sample B was also more compared to A, see **Fig. 10**.

4. Conclusion

The vanadium-chromium carbides coating was produced in-situ by powder injection of FeCrV15 powder through laser additive manufacturing on a steel baseplate for tillage application. A 3kW Continuous Wave (CW) IPG Fibre laser system with 1200 W laser beam power, 8 mm/s scanning speed and 5 g/min powder flow rate was utilised in the experiment. The effect of extra chromium addition at 0.4 g/min powder flow was also investigated on the developed coatings' microstructure, hardness and wear performance. This work has been attempted to clarify the formation mechanism and to analyse the developed coating. The significant outcomes are as follow:

- The clad coating on the steel substrate showed an incredible metallurgical bonding with no defect.
- The distribution of precipitated carbide particles and their grain sizes increase steadily from the clad-substrate interface to the top surface of the clads.
- The extra chromium addition increased the austenitic iron formation, reduced the concentration of the precipitated carbides and resulted in a much bigger grain formation of phases present, which lowered the grain boundary density leading to a reduced hardness of 553 HV for FeCrV15+Cr, compared to 835 HV for FeCrV15; which are significantly higher than 170 HV for the steel substrate.
- The FeCrV15 coating displayed an improved, multiple times wear-resistant capacity when contrasted with the FeCrV15+Cr. This excellent resistance is credited to the increased concentration of VC–Cr_3C_3 particles and increased grain boundary density due to the grain refinement of FeCrV15 coating, which are emphatically fortified in the matrix.

Declarations

Ethics approval

Not applicable.

Consent to participate

Not applicable.

Consent to publish

All authors consent that this manuscript should be published by the Applied Physics A: Materials Science and Processing.

Credit author statement

Basiru Aramide conceptualized the idea, formulated the research goals, and aims developed the design methodology and the creation of models, designed the study, and wrote the original draft of the manuscript.

Rotimi Sadiku supervised and assisted with the provision of study materials, editing and reviewing the original draft of the manuscript.

Patricia Popoola supervised, taught, and managed the literature review searches, and the investigation processes.

Sisa Pityana supervised and assisted with the technicality of the work,

Tamba Jamiru supervised and helped with the editing and reviewing of the draft.

Credit authorship contribution statement

Basiru Aramide: Conceptualization, Data curation, Formal analysis, Investigation, Methodology, Writing - original draft.

Rotimi Sadiku: Project administration, Resources, Supervision, Writing - review & editing.

Patricia Popoola: Project administration, Resources, and Supervision.

Sisa Pityana: Project administration, Resources, Supervision, Validation.

Tamba Jamiru: Project administration, Supervision.

Funding

This work is funded by the Tshwane University of Technology, Pretoria South Africa.

Declaration of Competing Interest

The authors declare that there is no known contending monetary interests or individual connections that might have influenced this work.

Availability of data and material

Not applicable.

Code availability

Not applicable.

Acknowledgement

The authors acknowledge the financial support from Tshwane University of Technology (TUT), Pretoria, South Africa, without which this work would not have been possible. The authors appreciate the effort of Samuel Skhosane, Paul Lekoadi and Thembi Dlamini of the National Laser Centre (Laser Enabled Manufacturing Resource Group), Council for Scientific and Industrial Research (CSIR) for their assistance with the machine.

References

1. Singh, J., S.S. Chatha, and B.S. Sidhu, *Abrasive wear behavior of newly developed weld overlaid tillage tools in laboratory and in actual field conditions.* Journal of Manufacturing Processes, 2020. **55**: p. 143-152.
2. Aramide, B., et al., *Improving the durability of tillage tools through surface modification—a review.* The International Journal of Advanced Manufacturing Technology, 2021. **116**(1): p. 83-98.
3. Fernández, J.E., et al., *Materials selection to excavator teeth in mining industry.* Wear, 2001. **250**(1): p. 11-18.
4. Hrabě, P., M. Müller, and V. Hadač, *Evaluation of techniques for ploughshare lifetime increase.* Research in Agricultural Engineering, 2015. **61**(2): p. 72-79.
5. Natsis, A., G. Papadakis, and J. Pitsilis, *The Influence of Soil Type, Soil Water and Share Sharpness of a Mouldboard Plough on Energy Consumption, Rate of Work and Tillage Quality.* Journal of Agricultural Engineering Research, 1999. **72**(2): p. 171-176.
6. Scholl, M., R. Devanathan, and P. Clayton, *Abrasive and dry sliding wear resistance of Fe-Mo-Ni-Si and Fe-Mo-Ni-Si-C weld hardfacing alloys.* Wear, 1990. **135**(2): p. 355-368.
7. Kang, A.S., J.S. Grewal, and G.S. Cheema, *Effect of thermal spray coatings on wear behavior of high tensile steel applicable for tiller blades.* Materials Today: Proceedings, 2017. **4**(2): p. 95-103.
8. Hrabě, P. and M. Müller, *Research of overlays influence on ploughshare lifetime.* Research in Agricultural Engineering, 2013. **59**(4): p. 147-152.
9. Horvat, Z., et al., *Influence of ploughshare surface layers on ploughing efficiency.* Metalurgija, 2018. **57**(1-2): p. 125-127.
10. Aramide, B.P., et al., *Influence of Vanadium-Chromium Carbide on the Microstructure of Reinforced FeCrV15 Hardfacing during Laser Cladding Deposit.* Research Square, 2021.
11. Günther, K. and J.P. Bergmann, *Influencing Microstructure of Vanadium Carbide Reinforced FeCrVC Hardfacing during Gas Metal Arc Welding.* Metals, 2020. **10**(10): p. 1345.
12. Aramide, B.P., et al., *Addition of Chromium and its effect on the microstructure and mechanical properties of laser-coated high carbon ferrochrome alloy on mild steel.* Research Square, 2021.
13. Aramide, B., et al., *Influence of extra chromium addition on the microstructure, hardness, and corrosion behaviour of high carbon ferrochrome FeCrV15 deposited through laser cladding on steel baseplate for tillage application.* Surface Topography: Metrology and Properties, 2021. **9**(4): p. 045029.

14. Alamr, A., D.F. Bahr, and M. Jacroux, *Effects of alloy and solution chemistry on the fracture of passive films on austenitic stainless steel.* Corrosion Science, 2006. **48**(4): p. 925-936.
15. Bayer, R.G., *Wear Analysis for Engineers.* Industrial Lubrication and Tribology, 2008. **60**(4).
16. Wu, Q., et al., *Microstructure and wear behavior of laser cladding VC–Cr7C3 ceramic coating on steel substrate.* Materials & Design, 2013. **49**: p. 10-18.
17. Aramide, B., et al., *Influence of Vanadium-Chromium Carbide on the Microstructure of Reinforced FeCrV15 Hardfacing during Laser Cladding Deposit.* Journal of Materials Engineering and Performance, 2021.
18. Kocaman, E., et al., *The influence of chromium content on wear and corrosion behavior of surface alloyed steel with Fe(16−x)Crx(B,C)4 electrode.* Engineering Science and Technology, an International Journal, 2021. **24**(2): p. 533-542.
19. Venkatesh, B., K. Sriker, and V.S.V. Prabhakar, *Wear Characteristics of Hardfacing Alloys: State-of-the-art.* Procedia Materials Science, 2015. **10**: p. 527-532.
20. Ralston, K.D. and N. Birbilis, *Effect of Grain Size on Corrosion: A Review.* Corrosion, 2010. **66**(7): p. 075005-075005-13.
21. Du, B., et al., *Laser cladding of in situ TiB2/Fe composite coating on steel.* Applied Surface Science, 2008. **254**(20): p. 6489-6494.
22. Darabara, M., G.D. Papadimitriou, and L. Bourithis, *Tribological evaluation of Fe–B–TiB2 metal matrix composites.* Surface and Coatings Technology, 2007. **202**(2): p. 246-253.

Figures

Figure 1

The Micrograph of a) High carbon ferrochrome FeCrV15 powder and b) Chromium powder.

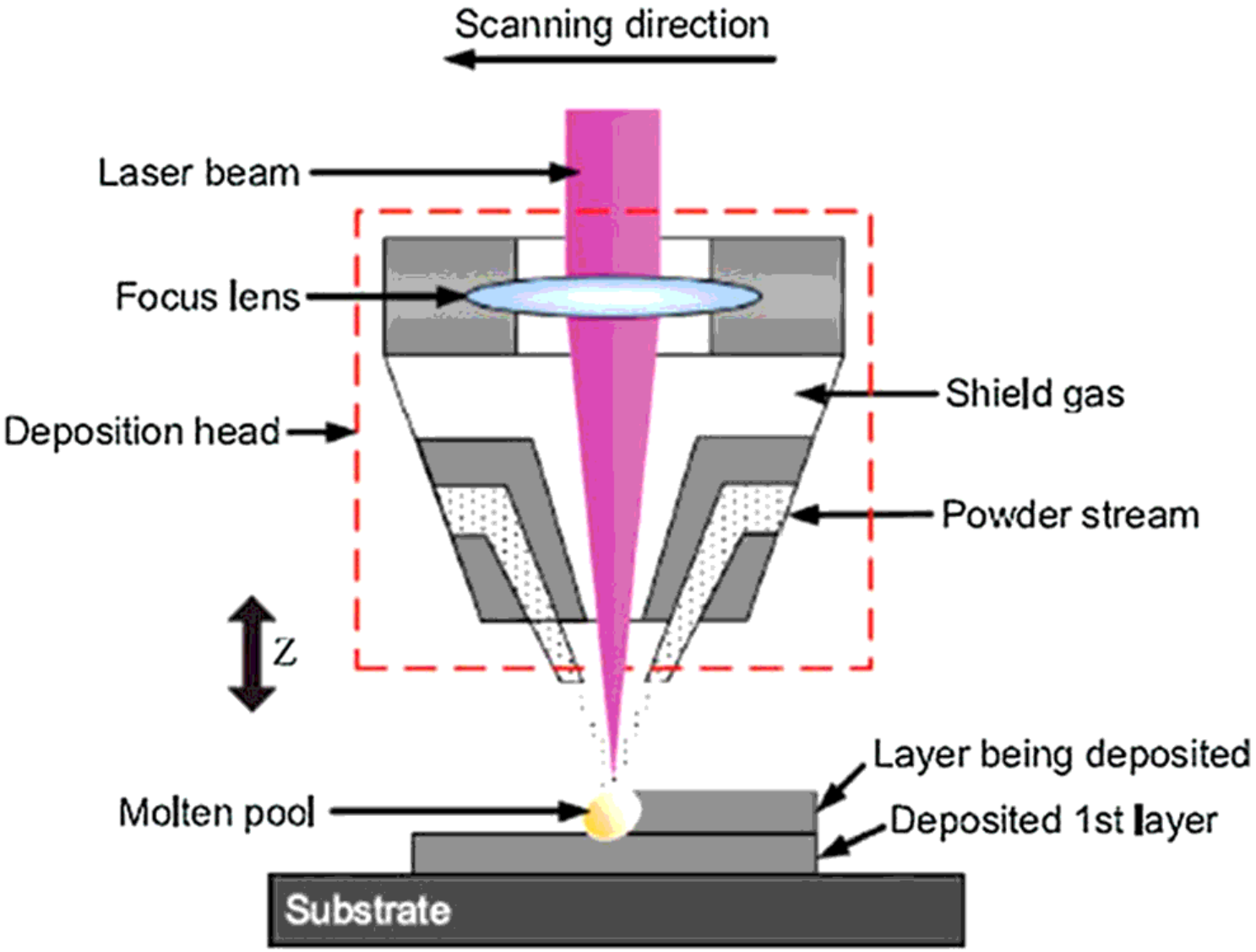

Figure 2

The representation of the laser head and process [2]

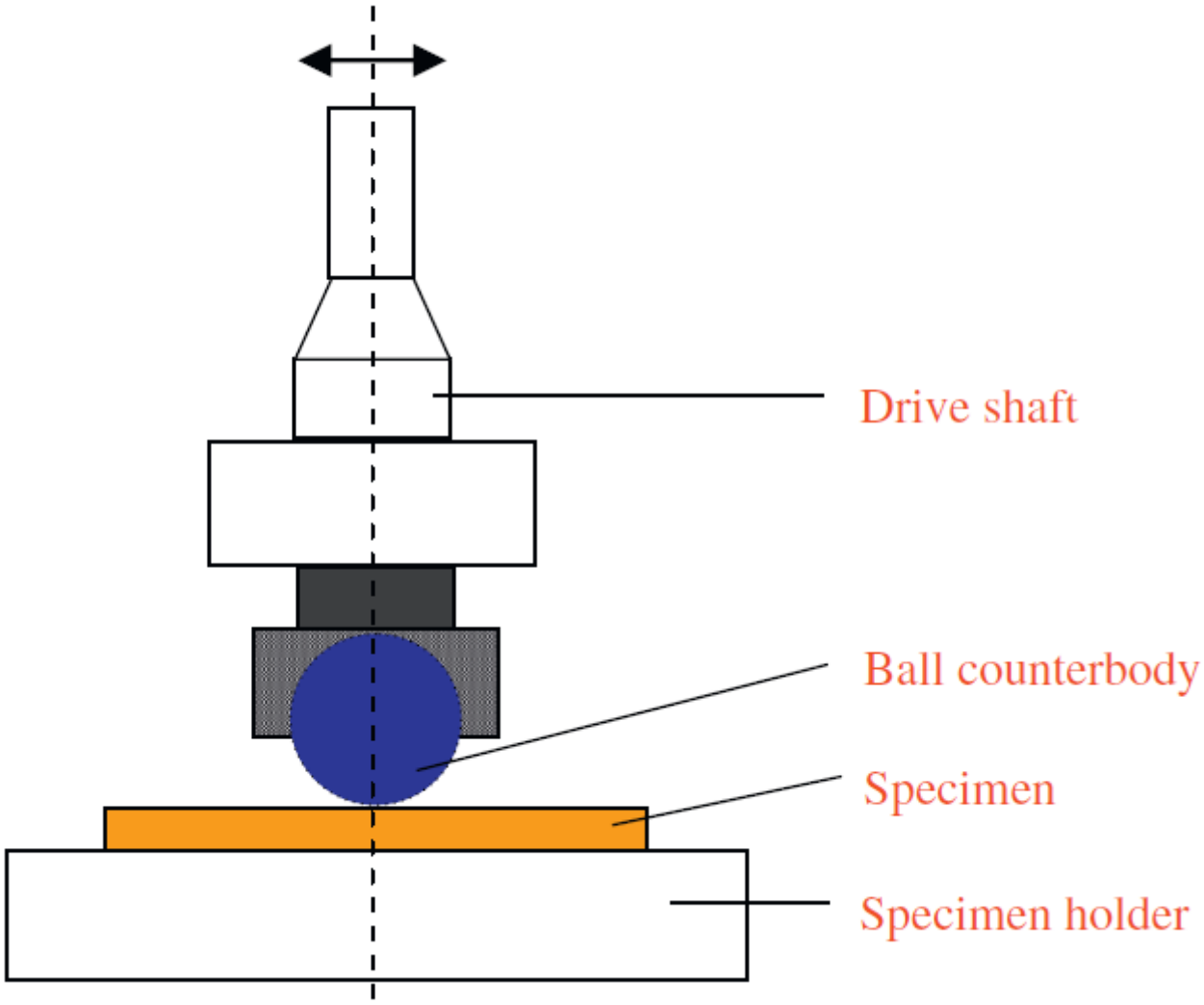

Figure 3

The schematic diagram of wear equipment [16]

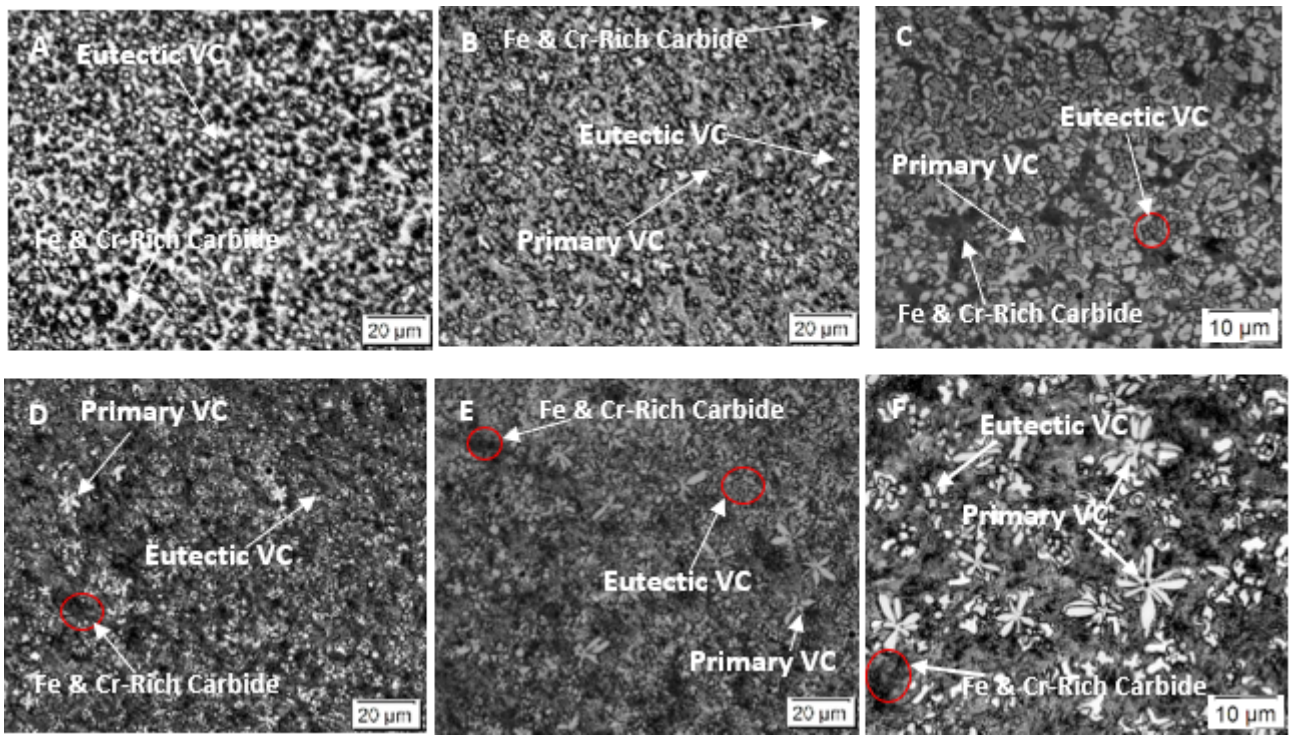

Figure 4

The micrographs of Samples A and B

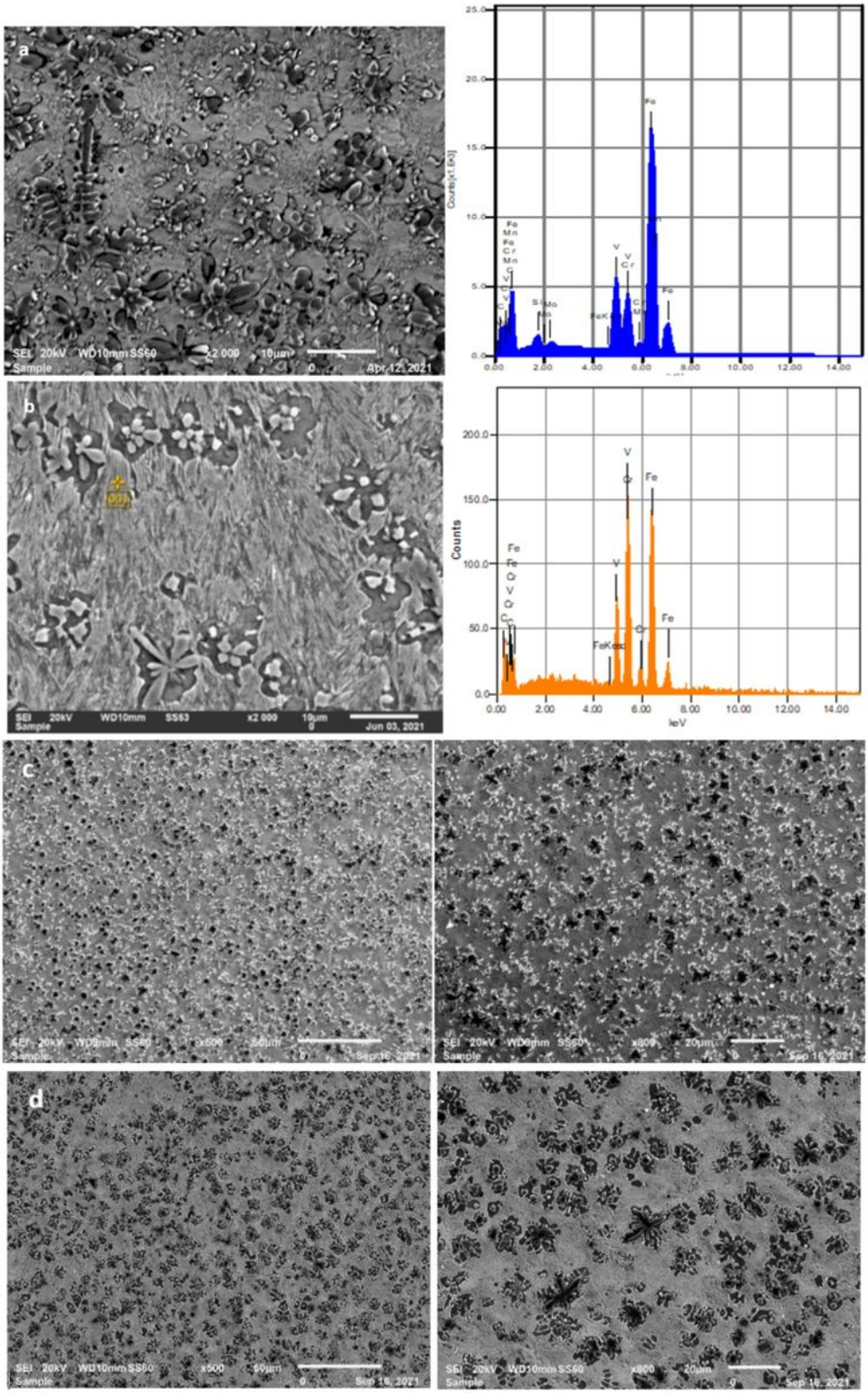

Figure 5

SEM/EDS images of the clad; a and c represent Sample A, while b and d Sample B.

Figure 6

X-ray diffractometry graph of the Samples

Figure 7

The microhardness profile of the coatings

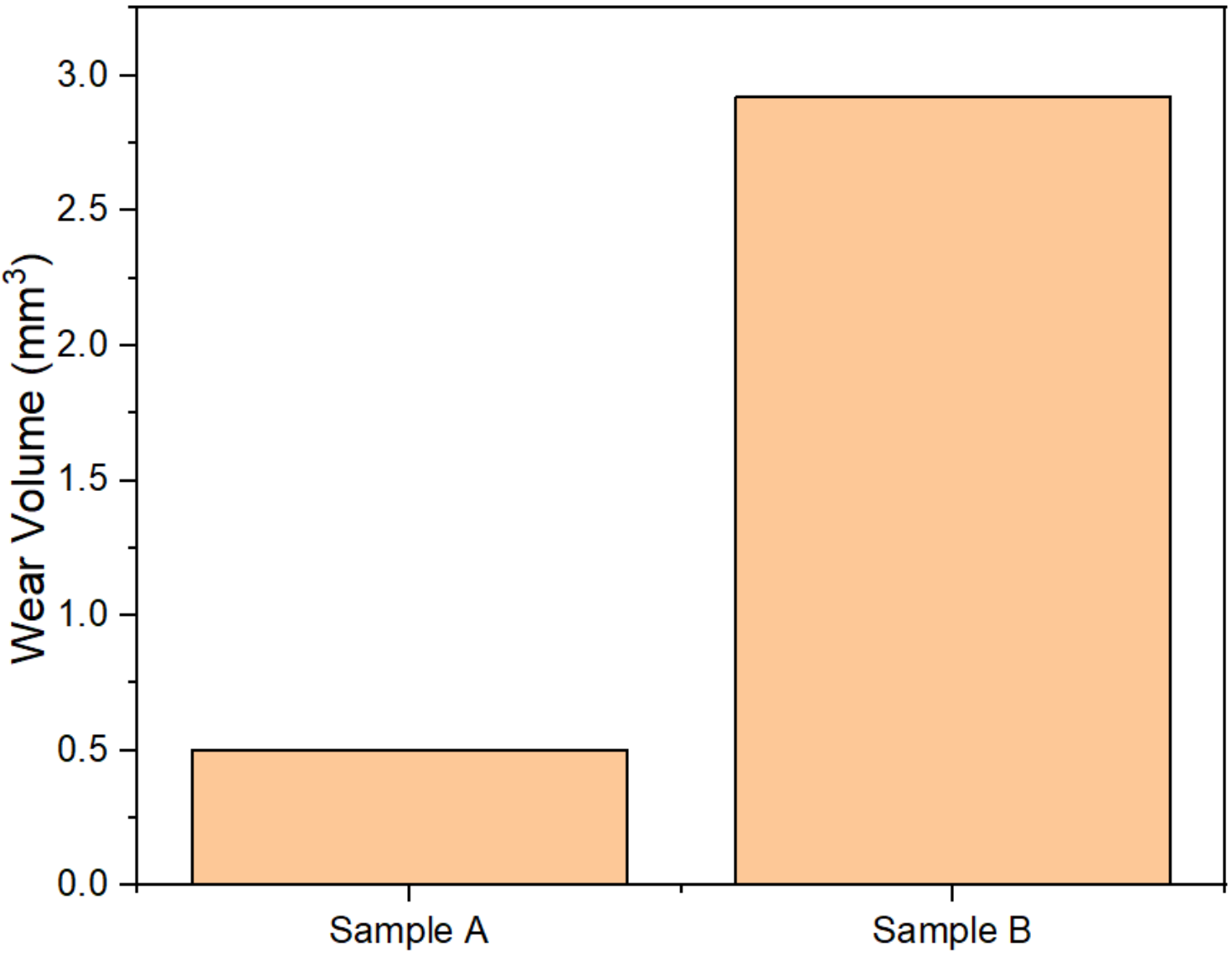

Figure 8

Wear volume loss of both coatings

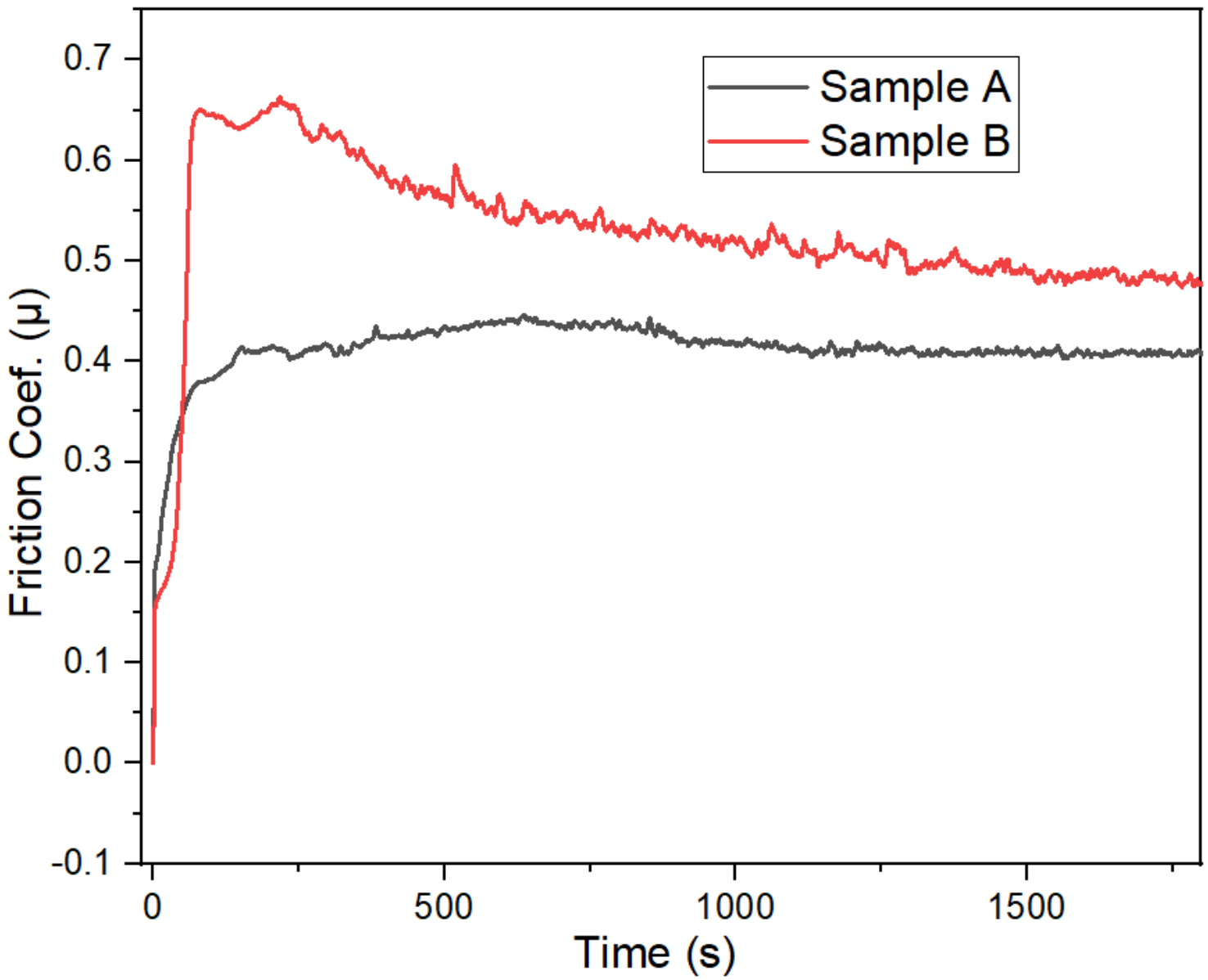

Figure 9

Friction coefficients as a function of time for the clad coating.

Figure 10

Micrographs of worn surfaces of both samples